

PENALIZED LEAST SQUARES METHODS FOR SOLVING THE EEG INVERSE PROBLEM

Mayrim Vega-Hernández, Eduardo Martínez-Montes,
José M. Sánchez-Bornot, Agustín Lage-Castellanos
and Pedro A. Valdés-Sosa

Cuban Neuroscience Center

Supplementary Material

1. Non-Convex Functions, Definitions and Some Properties

Definition 1.1. Let $p(\gamma) : \mathbb{R} \rightarrow \mathbb{R}$ a twice differentiable function in its domain. We say that $p(\gamma)$ is a convex (concave) function iff $p''(\gamma) \geq 0$ ($p''(\gamma) \leq 0$) for all $\gamma \in \mathbb{R}$.

Definition 1.2. Let $p(\gamma) : \mathbb{R} \rightarrow \mathbb{R}$ a twice differentiable function in its domain except in a subset $\Omega \in \mathbb{R}$. We say that $p(\gamma)$ is non-concave (non-convex) function iff $p(\gamma)$ is convex (concave) in $\gamma \in \mathbb{R} \setminus \Omega$. Note: This definition includes the case of even functions which are concave in $(0, +\infty)$ and have a singularity in its origin.

As discussed by Fan and Li (2001), the non-convex (with singularity in the origin) penalty functions are good options for variable selection in linear models since they may provide estimators with properties such as:

Sparsity: The resulting estimator is a thresholding rule, which automatically sets small estimated coefficients to zero to reduce model complexity. The solution is characterized by having a very small number of nonzero coefficients.

Unbiasedness: The resulting estimator is nearly unbiased when the true coefficient is large to avoid unnecessary modeling bias ($E(\hat{\mathbf{j}}) \approx \mathbf{j}$).

Continuity: The resulting estimator is continuous in some sense in order to reduce instability in model prediction.

2. Quadratic Inverse Solution Methods and Definitions of Different Smoothing Operators

Table 1. Some quadratic inverse solution methods and corresponding abbreviations.

Methods	Abbreviation (reference)
Minimum Norm	MN (Hämäläinen and Ilmoniemi (1994))
Weighted Minimum Norm	WMN (Pascual-Marqui (1999))
Backus and Gilbert method	BG (Backus and Gilbert (1967))
LOW-Resolution Electromagnetic TomogrAphy	LORETA (Pascual-Marqui, Michel, Lehmann (1994))
Variable Resolution Electromagnetic TomogrAphy	VARETA (Bosch-Bayard, Valdés-Sosa, Virués-Alba, Aubert-Vázquez, John, Harmony, Riera-Díaz, Trujillo-Barreto (2001))
Weighted Resolution OPTimization	WROP (Grave de Peralta, González, Hauk, Spinelli, Michel (1997))
Local AUtoRegressive Average	LAURA (Grave de Peralta, González, Lantz, Michel and Landis (2001))
standardized Low Resolution Electro-magnetic TomogrAphy	sLORETA (Pascual-Marqui (2002))

Table 2. Smoothing operators used in penalized least squares regression.

Name	Notation	Matrix
Identity	\mathbf{I}_n	$\begin{bmatrix} 1 & 0 & 0 & 0 \\ 0 & 1 & \cdots & 0 \\ 0 & \cdots & \cdots & 0 \\ 0 & 0 & 0 & 1 \end{bmatrix}$
1D gradient	\mathbf{D}_n^1	$\begin{bmatrix} 1 & -1 & 0 & \cdots & 0 \\ 0 & 1 & -1 & \cdots & 0 \\ & & \cdots & & \\ 0 & \cdots & 0 & 1 & -1 \\ 0 & \cdots & 0 & 0 & 1 \end{bmatrix}$
2D gradient	\mathbf{D}_{nm}^2	$\begin{bmatrix} \mathbf{I}_n \otimes \mathbf{D}_m^1 \\ \mathbf{D}_n^1 \otimes \mathbf{I}_m \end{bmatrix}$
2D laplacian	\mathbf{L}_{nm}^2	$\mathbf{D}_n^1 \otimes \mathbf{D}_m^1$
3D gradient	\mathbf{D}_{nmp}^3	$\begin{bmatrix} \mathbf{I}_n \otimes \mathbf{I}_m \otimes \mathbf{D}_p^1 \\ \mathbf{I}_n \otimes \mathbf{D}_m^1 \otimes \mathbf{I}_p \\ \mathbf{D}_n^1 \otimes \mathbf{I}_m \otimes \mathbf{I}_p \end{bmatrix}$
3D laplacian	\mathbf{L}_{nmp}^3	$\mathbf{D}_n^1 \otimes \mathbf{D}_m^1 \otimes \mathbf{D}_p^1$

3. Simulated Data Sets

Table 3. Talairach coordinates of the maximum values of the 20 simulated PCD. Five simulations were prepared in four different regions inside the brain.

Region	Coordinates			Region	Coordinates		
	x	y	z		x	y	z
Cingulate	-8	48	12	Poscentral	20	-43	68
	6	48	12		13	-43	68
	6	48	5		27	-43	68
	-8	48	5		20	-36	68
	-8	55	12		13	-43	61
Temporal	34	-8	-37	Occipital	-22	-99	-2
	41	-8	-37		-29	-99	-2
	34	-8	-30		-15	-99	-2
	34	-8	-44		-22	-99	5
	34	-15	-37		-22	-99	-9

Table 4. Mean values of optimal regularization parameters (λ), a corresponding GCV and a coefficient of variation (Coeff) for simulated data.

	OCCIPITAL			POSCENTRAL		
	λ	Min GCV	Coeff	λ	Min GCV	Coeff
MN	9.59×10^{-9}	7.09×10^{-13}	1.02	9.59×10^{-9}	7.22×10^{-13}	0.60
LORETA	3.02×10^{-2}	5.24×10^{-6}	1.00	1.53×10^{-2}	4.94×10^{-6}	0.66
RFused	7.13×10^{-17}	4.07×10^{-12}	1.02	7.13×10^{-17}	4.14×10^{-12}	0.61
LASSO	4.26×10^{-16}	5.07×10^{-11}	0.64	1.11×10^{-16}	2.13×10^{-10}	0.91
LFusion	1.36×10^{-16}	6.14×10^{-10}	0.59	2.99×10^{-16}	1.28×10^{-8}	0.44
LFused	3.99×10^{-11}	2.05×10^{-9}	0.60	2.29×10^{-10}	4.50×10^{-8}	0.45
SCAD L	1.02×10^{-13}	1.44×10^{-23}	0.58	1.02×10^{-13}	1.44×10^{-23}	0.35
ENET L	8.64×10^{-12}	1.73×10^{-8}	0.44	1.11×10^{-13}	1.58×10^{-8}	0.18

	CINGULATE			TEMPORAL		
	λ	Min GCV	Coeff	λ	Min GCV	Coeff
MN	9.59×10^{-9}	5.42×10^{-13}	0.69	9.59×10^{-9}	2.91×10^{-13}	0.59
LORETA	1.12×10^{-2}	5.23×10^{-6}	0.76	1.26×10^{-2}	1.25×10^{-6}	0.92
RFused	7.13×10^{-17}	3.11×10^{-12}	0.69	7.13×10^{-17}	1.54×10^{-12}	0.59
LASSO	5.49×10^{-16}	1.04×10^{-9}	0.62	1.62×10^{-16}	5.53×10^{-10}	0.52
LFusion	8.30×10^{-16}	6.89×10^{-10}	0.27	4.22×10^{-17}	3.00×10^{-10}	0.41
LFused	3.71×10^{-11}	2.21×10^{-9}	0.32	8.99×10^{-7}	8.97×10^{-8}	0.19
SCAD L	6.96×10^{-14}	1.07×10^{-25}	0.76	1.08×10^{-10}	8.54×10^{-11}	0.72
ENET L	3.75×10^{-10}	4.21×10^{-8}	0.16	6.04×10^{-14}	4.15×10^{-8}	0.32

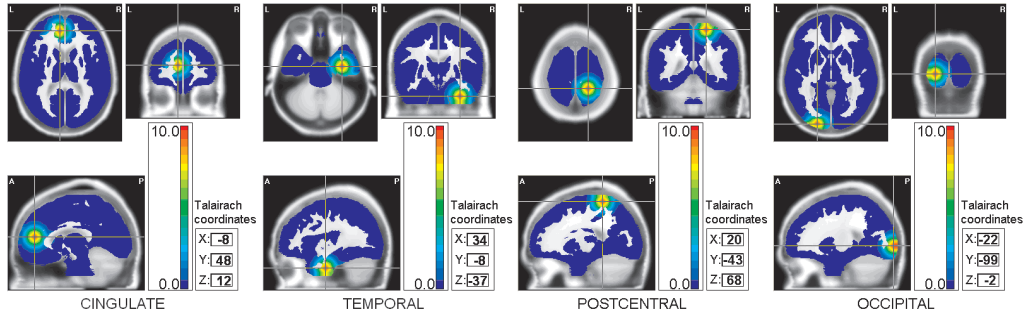


Figure 3.1. Four simulated PCD as three-dimensional Gaussians with maxima in different regions inside the brain. In all cases the amplitude and width of the gaussians are fixed to 10 nA/mm^2 and 10 mm respectively. The coordinates of the maxima are shown in Talairach's system (Talairach and Tournoux (1988)).

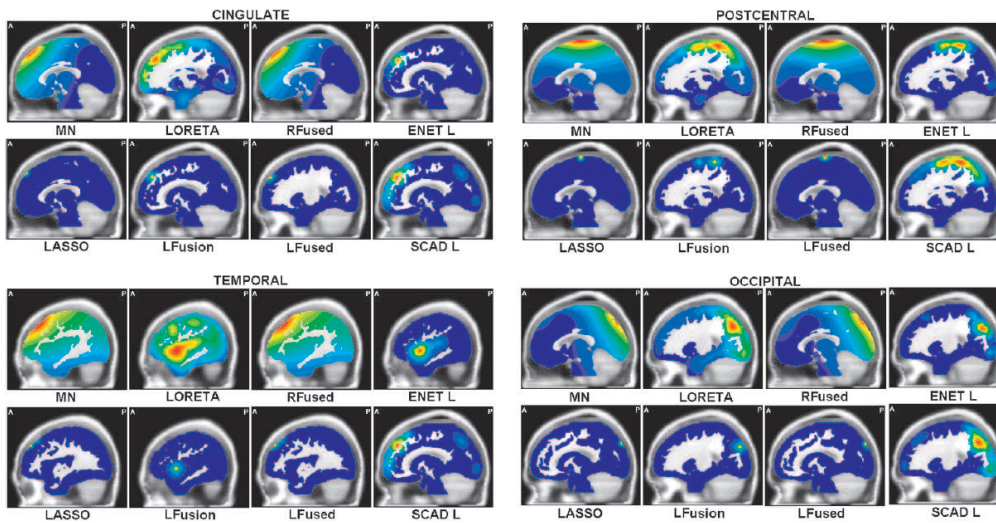


Figure 3.2. Sagittal views of eight different inverse solutions for the four simulated 3D Gaussian PCD.

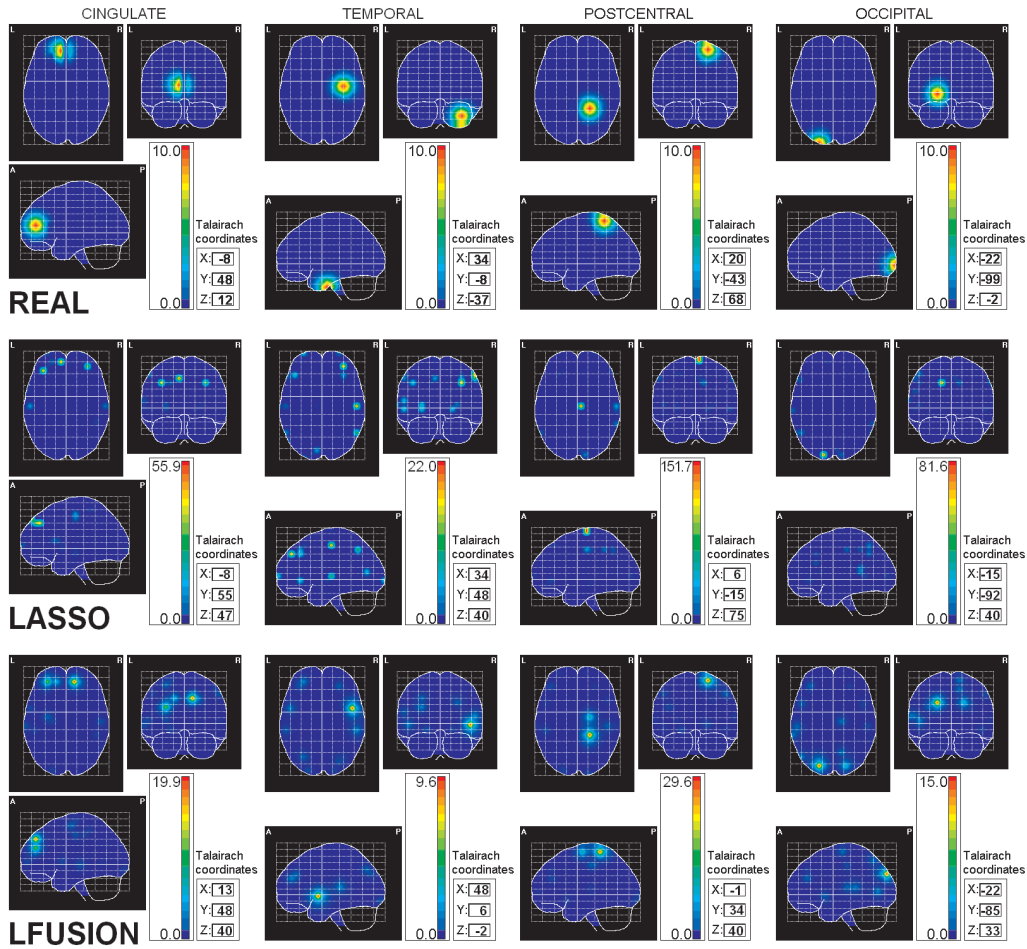


Figure 3.3. (Top) Four simulated PCD as three-dimensional Gaussians with maxima in different regions inside the brain (Figure 3.1). LASSO and LFUSION (middle and bottom rows, respectively) show sparse solutions with some “ghost sources”. The coordinates of the maxima are shown in Talairach’s system (Talairach and Tournoux (1988)).

4. Real Data

In order to explore the new properties offered by the proposed inverse solutions in the case of real neuroscience data, we performed a source localization analysis of the test data provided by the EEGLAB Toolbox (Delorme and Makeig (2004)), which is freely available at <http://sccn.ucsd.edu/eeglab/eeglabtut.html>. This data set corresponds to an experiment designed for the study of the attention modulation of the early visual components evoked by the stimuli presented in different parts of the visual field (Townsend, Harris and Courchesne (1996)).

Experimental design: ERPs were recorded from subjects who attended to randomized sequences of filled round or square disks appearing briefly inside one of five empty squares that were constantly displayed 0.8 cm above a central fixation cross (Fig. 4A). During each 76 sec block of trials, one of the five outlines was colored green, and the other four were blue. The green square marked the location to be attended. This location was counterbalanced across blocks. One hundred single stimuli (filled white circles in one condition, filled circles and squares in a second) were displayed for 117 msec within one of the five empty squares in a pseudorandom sequence with interstimulus intervals of 250–1000 msec (in four equiprobable 250 msec steps).

Subjects were instructed to maintain fixation on the central cross while responding only to stimuli presented in the green-colored (attended) square. In the “detection” task condition, all stimuli were filled circles, and subjects were required to press a right-hand held thumb button as soon as possible after stimuli presented in the attended location (Fig. 4B). Thirty blocks of trials were collected from each subject, yielding 120 target and 480 nontarget trials at each location. Subjects were given 1 min breaks between blocks. In the “discrimination” task condition, 75% of the presented stimuli were filled circles, the other 25% filled squares. Subjects were required to press the response button only in response to filled squares appearing in the attended location (Figure 4C) and to ignore filled circles.

These experiments were designed and run to study the attentional enhancement of early visual components P1 and N1 (positive and negative peaks occurring between 100 and 200 msec) evoked by stimuli presented in different parts of the visual field (Townsend, Harris and Courchesne (1996)).

Others details of the experiment and processing of the data can be found in Makeig, Westerfield, Jung, Covington, Townsend, Sejnowskii and Courchesne (1999) and in Makeig, Westerfield, Jung, Enghoff, Townsend, Courchesne and Sejnowskii (2002).

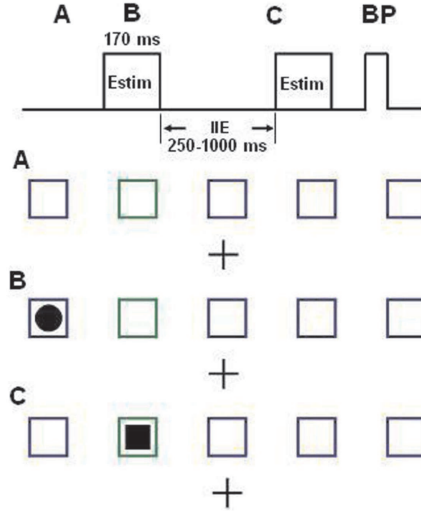


Figure 4. Schematic view of the task. The top trace shows the time line of a typical trial. BP, Button press. A, Screen before stimulation. The cross is the fixation point, and the lightly shaded box is the attended location during the ensuing 76 sec block. B, Appearance of a filled circle stimulus at an unattended location; no response required. C, Appearance of a filled square at the attended location in the discrimination task; button press required.

Table 5. Optimal values for the regularization parameters (λ) and corresponding GCV for real data.

Method	λ	Mín GCV
LORETA	$7.991 \cdot 10^{-7}$	$9.00 \cdot 10^{-3}$
ENETL ($\frac{\lambda_1}{\lambda_2} = 10^0$)	$9.068 \cdot 10^{-13}$	$6.80 \cdot 10^{-4}$
ENETL ($\frac{\lambda_1}{\lambda_2} = 10^1 - 1$)	0.5856	$3.34 \cdot 10^{-2}$
ENETL ($\frac{\lambda_1}{\lambda_2} = 10^2 - 1$)	$5.649 \cdot 10^{-10}$	0.1336
ENETL ($\frac{\lambda_1}{\lambda_2} = 10^3 - 1$)	$1.880 \cdot 10^{-8}$	$2.20 \cdot 10^{-2}$
ENETL ($\frac{\lambda_1}{\lambda_2} = 10^4 - 1$)	$1.880 \cdot 10^{-6}$	$2.30 \cdot 10^{-3}$
LFusion	$1.107 \cdot 10^{-12}$	$3.78 \cdot 10^{-7}$

References

- Backus, G. and Gilbert, F. (1967). Numerical applications of a formalism for geophysical inverse problems. *Geophys J. R. Astron Soc.* **13**, 247-276.
- Bosch-Bayard, J., Valdés-Sosa, P., Virués-Alba, E., Aubert-Vázquez, E., John, E. R., Harmony, T., Riera-Díaz, J. and Trujillo-Barreto, N. (2001). 3D statistical parametric mapping of

- variable resolution electromagnetic tomography (VARETA). *Clin. Electroencephal.*, **32**, 47-66.
- Delorme, A. and Makeig, S. (2004). EEGLAB: an open source toolbox for analysis of single-trial EEG dynamics including independent component analysis. *J Neurosci. Meth.* **134**, 9-21.
- Fan, J. Q. and Li, R. Z. (2001). Variable selection via nonconcave penalized likelihood and its oracle properties. *J. Amer. Statist. Assoc.* **96**, 1348-1360.
- Grave de Peralta, R., González, S. L., Hauk, O., Spinelli, L., Michel, C. M. (1997) A linear inverse solution with optimal resolution properties: WROP. *Biomedical Engineering (Biomedizinische Technik)*, **42**, 1, 53-56.
- Grave de Peralta, R., González, S., Lantz, G., Michel, C. M. and Landis, T. (2001). Non-invasive Localization of Electromagnetic Epileptic Activity. I. Method Descriptions and Simulations. *Brain Topogr.*, **14**, 2, 131-137.
- Hämäläinen, M. S. and Ilmoniemi, R. J. (1994). Interpreting magnetic fields of the brain: minimum norm estimates. *Med. Biol. Eng. Comput.* **32**, 35-42.
- Makeig, S., Westerfield, M., Jung, T.-P., Covington, J., Townsend, J., Sejnowskii, T. J. and Courchesne, E. (1999). Functionally independent Components of the Late Positive Event-Related Potential during Visual Spatial Attention. *J. Neurosci.* **19**, 2665-2680.
- Makeig, S., Westerfield, M., Jung, T.-P., Enghoff, S., Townsend, J., Courchesne, E. and Sejnowskii, T. J. (2002). Dynamic Brain Sources of Visual Evoked Responses. *Science*, **295**, 690-694.
- Pascual-Marqui, R. D., Michel, C. M. and Lehmann, D. (1994). Low resolution electromagnetic tomography: a new method for localizing electrical activity in the brain. *Int. J. Psychophysiol* **18**, 49-65.
- Pascual-Marqui, R. D. (1999). Review of Methods for solving the EEG Inverse Problem. *Inter. J. Bioelectromagnetism* **1**, 75-86.
- Pascual-Marqui, R. D. (2002). Standardize low resolution brain electromagnetic tomography (sLORETA). *Method Find Exp. Clin.* **24**, D, 5-12.
- Talairach, J. and Tournoux, P. (1988). Co-planar Stereotaxic Atlas of the Human Brain: 3-Dimensional Proportional System- an Approach to Cerebral Imaging. Theme Medical Publishers, New York.
- Townsend, J., Harris, N. S. and Courchesne, E. (1996). Visual attention abnormalities in autism: delayed orienting to location. *J. Int. Neuropsychology Society*, **2**, 541-550.

Neurostatistics Department, Cuban Neuroscience Center, Havana, Cub.

E-mail: mayrim@cneuro.edu.cu

Neurostatistics Department, Cuban Neuroscience Center, Havana, Cub.

E-mail: eduardo@cneuro.edu.cu

Neurostatistics Department, Cuban Neuroscience Center, Havana, Cub.

E-mail: bornot@cneuro.edu.cu

Neurostatistics Department, Cuban Neuroscience Center, Havana, Cub.

E-mail: agustin@cneuro.edu.cu

Neurostatistics Department, Cuban Neuroscience Center, Havana, Cub.

E-mail: peter@cneuro.edu.cu

(Received April 2007; accepted December 2007)